Journal of Archaeological Science 41 (2014) 333–348

Contents lists available at ScienceDirect

Journal of Archaeological Science

journal homepage: http://www.elsevier.com/locate/jas

Ten seconds in the field: rapid Armenian obsidian sourcing with portable XRF to inform excavations and surveys

Ellery Frahm [a, *], Beverly A. Schmidt [b], Boris Gasparyan [c], Benik Yeritsyan [c], Sergei Karapetian [d], Khachatur Meliksetian [d], Daniel S. Adler [b]

[a] Department of Archaeology, The University of Sheffield, Northgate House, West Street, Sheffield S1 4ET, United Kingdom
[b] Department of Anthropology, Old World Archaeology Program, University of Connecticut, 354 Mansfield Road, Unit 1176, Storrs, CT 06269, United States
[c] Institute of Archaeology and Ethnography, National Academy of Sciences, 15 Charents Street, Yerevan, Armenia
[d] Institute of Geological Sciences, National Academy of Sciences, 24 Baghramian Avenue, Yerevan, Armenia

ARTICLE INFO

Article history:
Received 19 May 2013
Received in revised form
30 July 2013
Accepted 12 August 2013

Keywords:
Obsidian
pXRF
Field methods
Armenia
South Caucasus
Palaeolithic archaeology

ABSTRACT

Armenia has one of the most obsidian-rich natural and cultural landscapes in the world, and the lithic assemblages of numerous Palaeolithic sites are predominantly, if not entirely, composed of obsidian. Recent excavations at the Middle Palaeolithic cave of Lusakert 1 recovered, on average, 470 obsidian artifacts daily. After sourcing more than 1700 artifacts using portable XRF (pXRF) in our field house, our team sought to shift pXRF-based obsidian sourcing into the field itself, believing that the geological origins of artifacts would be useful information to have on-site during an excavation or survey. Despite increasing use of portable instruments, previous studies have principally focused on collections in museums and other archives, and as a result, obsidian sourcing has remained embedded in post-excavation studies. One critical factor in the uptake of obsidian sourcing in the field is the time needed to measure each artifact, frequently 2–6 min in previous studies. Here we report our two methods of obsidian sourcing, including source matching done automatically by the pXRF instrument's onboard software, in only 10 s. Our tests with Armenian geological specimens and Palaeolithic artifacts demonstrate the high efficacy of our two methods, which are sufficiently fast to become syncopated with our excavation and survey activities. By reducing measurement times from a mode of 300 s in recent studies to just 10 s, here we show how (and why) to shift pXRF-based obsidian sourcing from the context of "white lab coats" to that of "muddy boots."

© 2013 Elsevier Ltd. All rights reserved.

1. Introduction

Although smaller than Belgium or the state of Maryland, Armenia has more than a dozen obsidian-bearing volcanic centers, resulting in one of the most obsidian-rich natural and cultural landscapes in the world. At numerous Palaeolithic sites, obsidian comprises the majority, if not the entirety, of the lithic assemblage. This is the case at two sites recently excavated by the Hrazdan Gorge Palaeolithic Project (Adler et al., 2012): Nor Geghi 1, an open-air Lower Palaeolithic site, and Lusakert 1, a Middle Palaeolithic cave site (Fig. 1). Their lithic assemblages are more than 99% obsidian. At Lusakert 1, in particular, after four excavation seasons (2008–2011), 13,970 obsidian artifacts have been recovered (excluding 5970 fragments smaller than 25 mm) from 11.9 m^3 of sediment. That is, 1174 obsidian artifacts were recovered per cubic meter. On average, 470 obsidian artifacts were excavated daily with spatial data recorded by two Leica total stations.

In 2011, the project began a new program of obsidian studies, including artifact sourcing as well as source surveys and characterization. During the 2012 season, we analyzed over 1700 artifacts in our field house using portable X-ray fluorescence (pXRF). We established that the Nor Geghi 1 and Lusakert 1 assemblages were both approximately 93% obsidian from Gutansar (sometimes spelled as Gutanasar), the nearest volcanic center with abundant obsidian resources. The remainder came from numerous sources throughout Armenia, including Hatis, Pokr and Mets Arteni, Pokr Sevkar, Geghasar, and the Tsakhkunyats sources. Publications on these findings, included detailed source and spatial data, are currently in preparation. The focus of this paper is a methodological development that arose out of our work, specifically a desire to have obsidian source information available on-site. The methods we document here will be deployed in future seasons, becoming a

* Corresponding author. Tel.: +44 74 0299 0202.
E-mail addresses: elleryfrahm@gmail.com, e.frahm@sheffield.ac.uk (E. Frahm).

0305-4403/$ – see front matter © 2013 Elsevier Ltd. All rights reserved.
http://dx.doi.org/10.1016/j.jas.2013.08.012

Fig. 1. Armenia obsidian sources (black circles) included in this study, archaeological sites referenced in the text (black squares), and source complexes (dashed lines) as conceptualized in the tests. Localities with different names but identical compositions are represented by a single dot (e.g., Djraber, Gyumush, Fontan, etc. localities of Gutansar). No attempt is made here to precisely represent the full primary and secondary distribution of the obsidians. For this study, Syunik complex specimens did not include sources only recently surveyed by our team, such as Mijnek Satanakar, Pokr Satanakar, and Merkasar. Although not conceptualized as such for this study, Gutansar and Hatis can be considered the Hrazdan-Kotayk group, while Khorapor is part of the Vardenis group. Apnagyugh-8 is unofficially known as Kmlo-2. Digital elevation data from SRTM3 (Shuttle Radar Topography Mission dataset version 3), and base map shared and modified under Creative Commons terms from Wikimedia Commons.

routine component of our excavation toolkit and constituting a key strategy in our approach to site surveys and assessments.

As hundreds of artifacts were sourced in our field house during the 2012 season and the results compared to the spatial data, it became clear to us (for reasons discussed in Section 2) that an artifact's geological origin would be useful information to have on-site during an excavation or survey. Our tests of visual classification yielded little success. Gutansar obsidian is highly variable in appearance, and as Table 1 shows, any "exotic" artifacts from other sources were overlooked and grouped into types with Gutansar artifacts. Thus, we began our efforts to develop methods for shifting pXRF from our field house into the field itself. As discussed in Section 2.4, pXRF-based obsidian sourcing has hitherto been largely conducted in laboratories, museums, and field houses. Although our colleagues are using dust- and waterproof instruments with 10-h batteries, obsidian sourcing remains embedded in post-excavation studies and is rarely, if ever, done in the field.

A critical factor in the uptake of obsidian sourcing in the field is the time needed for each measurement. In recent pXRF-based obsidian studies (Table 2), analyses took 2–6 min. The most common duration is 5 min, corresponding to 12 artifacts per hour. Our excavations at Lusakert 1 yielded, on average, 70–80 artifacts per hour. Although this suggests a need for 45-s measurements, we aimed for 10 s so that these analyses could become syncopated with the excavation activities. Additionally, we deemed it was insufficient simply to conduct a measurement in that time. After 10 s, we wanted the instrument's built-in LCD to display an artifact's source so excavators and surveyors could instantly know the result.

Reducing measurements from a mode of 300 s to just 10 s and having the instrument's onboard software automatically do the data analysis is bound to raise challenging assumptions about the validity and reliability of our approach. We show that the technological capability to source obsidian artifacts rapidly on-site exists, but the methods to do so effectively were previously undeveloped. Our tests with Armenian geological specimens and Palaeolithic artifacts demonstrate the high efficacy of the two methods we report here.

2. Rationale for field-based sourcing

Obsidian artifact sourcing conducted rapidly on-site can transform the ways in which our discipline approaches subjects involving raw-material procurement, transport, and use as well as the organization of space and the identification of activity areas.

Table 1
Fifteen visual types of obsidian and 145 artifacts sorted by visual classification and by geochemical analysis. Gutansar obsidian is highly variable in appearance, so "exotic" artifacts from other obsidian sources were overlooked and grouped into types with a number of Gutansar artifacts. As a result, we deemed visual sorting to be unsatisfactory in this context.

	Black solid stripe	Coarse black	Coarse gray	Greasy black	Gray smooth stripes	Iridescent	Pale gray outline red	Solid smooth gray	Smokey clear	Smokey clear, striped	Smooth black	Solid red	Tiger stripe	Tiger stripe, major black	Tiger stripe, major red
Gutansar	3	3	9	6	3	15	7	7	8	32	9	12	7	11	8
Hatis										1					
Pokr Arteni													1		
Pokr Sevkar									1						
Tsakhkunyats 1										1					
Tsakhkunyats 3														1	

2.1. Note about "pXRF" terminology

In this paper, "pXRF" refers to the ruggedized instruments about the size and shape of a cordless drill. In contrast, some researchers (e.g., Craig et al., 2007; Liritzis and Zacharias, 2011; Speakman and Shackley, 2013) consider "pXRF" to include benchtop instruments that could be transported from an analytical laboratory to a similar context in a museum or field house. Such instruments have been used to good effect for sourcing obsidian artifacts (e.g., Cecil et al., 2007; Speakman et al., 2007; Liritzis, 2008). These systems, though, require a computer and electrical outlet, and they would not fare well outdoors. We focus on handheld analyzers designed for use in the field (e.g., geological exploration) and industrial settings (e.g., scrapyards, manufacturing).

2.2. Obsidian sourcing at an excavation

Obsidian sourcing at an archaeological site may yield insights that inform the excavation strategies. Consider, for instance, that most of the obsidian at our two sites originated from the nearest volcano, Gutansar; however, about 7% of the assemblages came from additional sources throughout Armenia. Some of the "exotic" artifacts are isolated finds of highly retouched tools, carried by hunter–gatherers across long distances. Others, though, occur as apparent scatters that suggest a few possibilities, including a worked nodule, a bundle or toolkit, or an occupation by a group that discarded their tools from a distant source as they made new ones. Recognizing such artifacts as they are unearthed might affect, for example, how an excavator approaches the lithic scatter, samples the stratum in that unit for dating or small finds, or interprets associated features. Such information at a subsequent time, whether years or days later, is useful but disconnected from these processes of excavation and field interpretation. The influence of excavation strategy on archaeological inquiry, especially with respect to sampling, is a matter of great significance in our discipline (e.g., Mathieu and Scott, 2004; Lyman, 2009).

There are examples of research designs in which recognizing changes in artifacts' origins, identified as they are unearthed, may affect how a site is excavated. On-site sourcing would lend itself to such topics as the integrity of "living floors" (Dibble et al., 1997; Enloe, 2006; Machado et al., 2013; Malinsky-Buller et al., 2011) and organization of space in palimpsest occupations (Feinman et al., 2007; Adler et al., 2003). For example, at Gatecliff Rockshelter in the Great Basin, archaeologists modified their excavation strategy in light of suspected living floors (Kelly and Thomas, 2012: 86–88). Specifically, when an artifact horizon was encountered, the strategy shifted from a vertical to horizontal one, opening large surfaces and following the stratigraphic levels. This change was accompanied by greater attention to small finds (i.e., changes in sieving practice and sampling criteria for lithic, faunal, and botanical evidence), including lithic debitage and the surrounding sediments. Without indicators of a new artifact horizon, particular strata of Gatecliff Rockshelter might have been excavated differently.

This is not to suggest that, should we encounter an artifact of Hatis obsidian at Lusakert 1 among a multitude from Gutansar, we would suddenly change our overall excavation strategy for the cave. It would be a mistake to pose anything so drastic. Rather, we propose adding obsidian sourcing to the observations available to excavators as they dig. Our methods offer a new way to make field observations because, as demonstrated by our tests of visual classification, volcanic source is one tangible aspect of the material culture not apparent while excavating. As a routine component of field practice, on-site obsidian sourcing may yield insights when such information would be immediately relevant to excavators and their interpretations.

Table 2
Measurement times in several recently published pXRF-based obsidian sourcing papers. These durations are consistent with Shackley's (2011) claim that XRF analysts tend to measure obsidian for 150–300 s.

	Duration (sec)
Golitko et al., 2010	60
Frahm et al., 2013	90
Goodale et al., 2012	120
Millhauser et al., 2011	120
Freund and Tykot 2011	180
Jia et al., 2010	180
Craig et al., 2010	200
Vázquez et al., 2011	200
Forster and Grave 2012	300
McCoy et al., 2011	300
Nazaroff et al., 2010	300
Tykot et al., 2011	300
Sheppard et al., 2011	360
Mean	*208*
Median	*200*
Mode	*300*

2.3. Obsidian sourcing on a field survey

We are also interested in insights from obsidian sourcing during surveys. Surveys are the principal means not only to search for and choose sites for excavation but also to reconstruct the distribution and organization of groups across the landscape. Obsidian sourcing during a survey may offer insights into settlement type, resource management, and other spatiotemporal patterns that inform how we approach surveys and document sites.

Consider Kuhn's (1995) provisioning strategies for mobile foragers. Resource planning must account for the frequency and predictability of moves, variety and abundance of foraging opportunities, and availability of replacement raw materials. Kuhn describes two approaches to maintain tool supplies: individual provisioning and place provisioning. Individual provisioning is a

strategy in which there is uncertainty about mobility, resource availability, and opportunities for reprovisioning with raw materials, while place provisioning is a strategy with lower mobility and greater predictability in resource availability and distribution. Thus, raw-material transport and management strategies differ based on mobility and landscape knowledge, and strategies on a particular landscape may vary diachronically due to climatic shifts.

Therefore, the ability to rapidly identify local and non-local obsidians during surveys has great interpretive potential. At sites just a short distance from an obsidian source, artifacts from only that source may indicate a strategy primarily influenced by place-provisioning. In contrast, sites with artifacts from diverse sources could reflect a predominance of individual provisioning. In reality, both provisioning strategies were almost always at work. For example, foragers may have used individual provisioning while traveling from the Syunik region to Gutansar, but while residing near Gutansar, they shifted to primarily place provisioning. It is not a simple either-or proposition, and the palimpsest issue remains. Thus, large assemblages sourced by pXRF and with detailed spatial and stratigraphic data are key to unveiling significant patterns.

Additionally, recognizing the spatial distributions of obsidians at a site could inform test pit locations or reveal different activity areas. Contrasting artifacts from the surface and levels of a test pit or trench add a temporal dimension, and correlating source data with artifact typology may uncover otherwise hidden diachronic changes in mobility between periods. At numerous open-air Palaeolithic sites in Armenia, little more is preserved than, in some instances, millions of obsidian artifacts. With a small team equipped with several pXRF instruments to cover a large area, working at such sites has become practical using the methods we report here, and the resulting datasets would be sufficiently nuanced to make meaningful behavioral interpretations.

2.4. pXRF and obsidian sourcing

Thus far pXRF-based obsidian studies have been primarily focused on sourcing artifacts at museums, universities, and archive facilities (i.e., collections previously beyond the reach of analytical techniques). Most studies have been conducted in museum labs and similar contexts (e.g., the Smithsonian's Museum Conservation Institute in Phillips and Speakman, 2009; Craig et al., 2010; Field Museum of Natural History's Elemental Analysis Facility in Golitko et al., 2010, 2012; Millhauser et al., 2011). For Craig et al. (2007), "*in situ* analysis" refers to measurements taken "where the artifacts are stored."

Despite increasing use of pXRF, obsidian sourcing remains embedded in post-excavation studies. When artifacts are sourced, they have been detached, often distantly, in time and space from their archaeological contexts. For example, Forster and Grave (2012) analyzed 26 Near Eastern artifacts, excavated during the 1930s, at an Australian museum. This division has been the dominant paradigm since the 1960s, and obsidian sourcing has been highly productive over the last five decades. Nevertheless, use of pXRF analyzers in laboratories clearly does not take full advantage of their capacities. Our aim is to shift obsidian sourcing from the realm of "white coats" in the controlled laboratory environment to "muddy boots" in the field.

3. Background

Before reporting the development and testing of our methods for rapid obsidian sourcing, we briefly discuss obsidian studies in Armenia and two different approaches to classification in obsidian sourcing, revealing two technique-based communities of practice.

3.1. Armenian obsidian sources

Given the abundance of obsidian sources in Armenia (Fig. 1), it is beyond the scope of this paper to discuss them in detail. Badalyan et al. (2004) synthesize Armenian sourcing studies prior to 2000, including that of Blackman et al. (1998) and research never fully published. Until recently, most source characterization was done with fission-track dating and neutron activation analysis (NAA; e.g., Oddone et al., 2000; Badalian et al., 2001; Chataigner et al., 2003; Kasper et al., 2004; Cherry et al., 2010; Meliksetian et al., 2010, 2013). Rarely XRF has been used (e.g., Keller et al., 1996 used both NAA and XRF). Chataigner and Gratuze (2013a) recently studied Armenian obsidians with laser ablation inductively coupled plasma mass spectrometry (LA-ICP-MS), characterizing most source complexes based on four to eight specimens each. Geologically focused studies include Keller et al. (1996) and Karapetian et al. (2001).

Relatively little archaeological data have been published regarding obsidian sourcing in Armenia, especially for the Palaeolithic. Most research has focused on the Neolithic to Bronze Age (e.g., Chataigner et al., 2003; Badalyan et al., 2004; Kasper et al., 2004; Chataigner and Barge, 2007; Cherry et al., 2010; Chataigner and Gratuze, 2013b). We are aware of obsidian sourcing at only one Palaeolithic site, Upper Palaeolithic Kalavan-1. Chataigner and Gratuze (2013b) have analyzed 18 artifacts and assigned them to Hatis (10), Gegham (4), Gutansar (3), and Satanakar in the Syunik complex (1). They also analyzed 20 artifacts from Mesolithic/proto-Neolithic Apnagyugh-8 (referred to by its unofficial name Kmlo-2) and attributed them to Gutansar (10), Tsakhkunyats (4), Arteni (3), Hatis (1), Gegham (1), and a source in the Kars province of north-eastern Turkey (1). Thus, hundreds of millennia of obsidian use by modern humans and other hominins has hitherto been largely unstudied in Armenia.

3.2. Approaches to classification in obsidian sourcing

There are two schools of thought regarding classification in obsidian sourcing, and our two methods reflect these distinct approaches. Neither approach is fundamentally correct, and in instances where both approaches successfully discern sources, there is no clear reason to choose one or the other (unless there is a benefit in time or cost).

The first approach is summarized concisely by Harbottle (1982): "the more elements, the better" (18). He sees sourcing as a form of taxonomy, applies taxonomic theory in his approach, and argues that classifications based on numerous traits are superior to those based on just a few. Harbottle cites the foundational book *Numerical Taxonomy* by Sneath and Sokal (1973), whose first taxonomic principle is: "the greater the content of information in the taxa of a classification and the more characters on which it is based, the better a given classification will be" (5). Thus, Harbottle claims that one tends to "get the best classifications out of the most information" (39). Similarly, Glascock (1992) maintains "it is advisable to use the information on all elements... to use the maximum amount of information" (17), citing Sneath and Sokal (1973). Consequently, Glascock and colleagues often use 20 or more elements in their source attributions (e.g., Ericson and Glascock, 2004; Glascock et al., 2007).

The second approach involves critical selection of elements. Hughes (1984) holds it "is not necessarily the case... that the inclusion of larger numbers of variables... results in a 'better' classification" (3). He contends poorly measured, redundant, or uninstructive elements should be excluded. Citing Hughes (1984), Shackley (1988) holds "improperly chosen" elements can "covertly skew the classification analysis" and maintains "the best course is to choose elements for analysis carefully" (763). Hence,

Shackley (1995) proposes "a rule of thumb... is to use the fewest variables necessary" (546), and he frequently relies on four key elements (e.g., Ba, Rb, Sr, Zr in Shackley, 2009; Fe, Mn, Zn, Zr in Negash and Shackley, 2006).

These approaches reflect different technique-linked communities of practice. Harbottle and Glascock are nuclear chemists who principally use NAA, while Hughes and Shackley have archaeological backgrounds and use XRF. What constitutes "standard practice" differs between the NAA and XRF communities. These differences are based on the strengths (and weaknesses) of each technique. NAA typically measures more than 20 trace elements in obsidian; however, early XRF instruments involved manually tuning a spectrometer to each element, so measuring fewer elements was desirable. By extension, methodological variations in pXRF use should be acceptable if those differences facilitate its strengths (e.g., field use).

4. Methods and materials

Our 10-s measurements take advantage of elements measured simultaneously with one X-ray filter, the development of faster detectors, and the relationship between measurement uncertainty and time. The tests we report here involved more than 500 geological specimens of Armenian obsidians and 154 Palaeolithic artifacts from Nor Geghi 1 and Lusakert 1.

4.1. Attaining 10-s measurements

Measurements in pXRF-based obsidian sourcing studies frequently take 2–6 min, and the most common duration is 5 min (Table 2). This is consistent with Shackley's (2011) claim that XRF analysts measure obsidian for 2.5–5 min. Using 2-min measurements, Millhauser et al. (2011) analyzed about 100 artifacts in an 8-h day. This pace is still too slow for use at sites where 400–500 obsidian artifacts are recovered daily. We require a method to process up to 80 artifacts per hour. On paper, this suggests 45-s measurements, but to be fully syncopated with the excavation activities, we aimed for 10 s.

Some measurement times in Table 2 involve the use of multiple X-ray filters inside the analyzer to measure different portions of the X-ray spectrum. The 90-s measurements in Frahm et al. (2013), for example, were two sequential 45-s measurements using different filters. One way to reduce measurement times is to focus on elements measured well using only one filter. For Niton instruments, it must be the "main" filter (i.e., the primary filter, which has a proprietary composition), which is used to fluoresce transition elements and measure a series of X-ray phenomena (e.g., Rayleigh and Compton scattering) to adjust for various physical effects (e.g., morphology, density) from a particular material or specimen.

Recent technological advancements in pXRF analyzers also enable shorter measurement times. Most important is the development of silicon drift detectors (SDD), which can attain the same precision 2–10 times faster than older silicon p-n diode (PN) detectors. The majority of prior studies have used analyzers with PN detectors (e.g., Craig et al., 2010; Golitko et al., 2010; Jia et al., 2010; Nazaroff et al., 2010; Millhauser et al., 2011; Sheppard et al., 2011; Vázquez et al., 2011; Forster and Grave, 2012). Therefore, our use of an SDD instrument enabled shorter counting times than those in previous studies.

Additionally, the relationship between the time and uncertainty of a measurement is not linear. Instead, uncertainty is inversely proportional to the square root of the number of X-ray counts and, thus, measurement time (Fig. 2). To cut uncertainty in half, measurement time must be quadrupled. Decreasing error from 10% to 2% necessitates a measurement 25 times longer. Precision quickly incurs a considerable time cost. To attain an average precision of 2.3% for six elements (Fe, Rb, Sr, Y, Zr, Ba), Giauque et al. (1993) measured for 1000 s (i.e., 16.7 min). If 10% relative error had been acceptable, each artifact could have been measured in less than a minute.

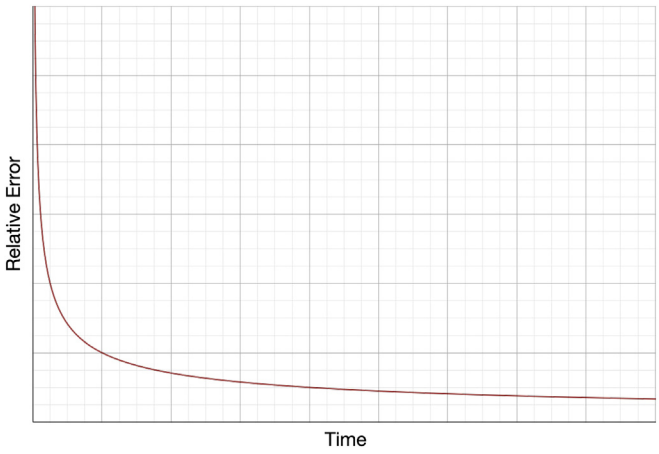

Fig. 2. The general trend for the relationship between the uncertainty of a measurement and the measurement time. It is an inverse square relationship. The units shown here are arbitrary, but this relationship holds for all elements and all forms of X-ray spectrometry.

4.2. Materials: instrument, artifacts, and geological specimens

Our tests used a Niton XL3t GOLDD+ pXRF analyzer. This instrument generates X-rays via a 50-kV tube with a silver anode, and it is outfitted with a silicon drift detector (SDD) that, as mentioned in Section 4.1, is 2–10 times faster than PN detectors. We have found that the XL3t GOLDD+ has, in practice, an X-ray resolution better than 155 eV (versus 180 eV, in practice, for the PN-based XL3t). Like other XRF instruments, Niton pXRF analyzers automatically monitor and adjust their tube currents (to a maximum of 200 μA for the GOLDD+) as a means to attain optimal X-ray count rates for a particular specimen or material. Additionally, when operated at 50 kV with the "main" filter, this instrument yields an X-ray flux about 60% greater than that of 40-kV tubes (flux increases with the square of voltage). With a higher flux, more X-rays enter a specimen and, in turn, excite more characteristic X-rays to measure.

More than 500 geological specimens of Armenian obsidians were used in these tests, and the majority was collected from the sources by our team. The tests also included 154 artifacts from Nor Geghi 1 (Lower Palaeolithic) and Lusakert 1 (Middle Palaeolithic). Artifacts were chosen prior to knowing their origins, which were identified before these tests.

All geological specimens and artifacts were previously analyzed using pXRF with more conventional procedures, including two-minute analyses, a test stand, and operation via a laptop. Analyses were conducted in "mining" mode, which uses fundamental parameters (FP) correction to adjust measurements for X-ray emission, absorption, fluorescence, and other phenomena. To convert the data into element concentrations, we initially used the factory-set calibration factors and subsequently applied linear-regression calibrations based on 24 obsidians analyzed by NAA and XRF at the University of Missouri's Research Reactor (MURR) and by electron microprobe analysis (EMPA) at the University of Minnesota. These data will be detailed in a publication, currently in preparation, regarding obsidian sources important at sites along the Hrazdan River.

5. Method 1: spectrum matching and χ^2 fits

Our first method makes use of the pXRF algorithms to automatically identify metal alloys, and it follows Harbottle's approach to classifying obsidian artifacts. Specifically, 24 elements are compared in a specimen and reference library using χ^2 fits calculated in realtime.

5.1. Using the "Spectral Fingerprints" algorithms

One of the most common uses of pXRF is automated identification of alloys and metal grades in as little as 3–5 s. These instruments are routinely used in metal scrapyards to quickly identify, for example, different grades of stainless steel. In some manufacturing fields, including the aerospace and petrochemical industries, pXRF is used for alloy verification of every component as part of their quality assurance measures. The onboard software compares measurements to an integrated library of more than 400 alloys and displays the closest match in realtime on the built-in LCD. This process is known as positive material identification (PMI). Every day thousands of pXRF analyzers are used in commercial PMI applications, and a single worker can take as many as 1000 measurements during an eight-hour shift.

These algorithms can also be used with other materials and custom libraries. In the Niton software, this is called *Spectral Fingerprint* mode. First one uses the *Teach Fingerprint* routine to record spectra from reference materials and create a custom library. Each measurement takes 60 s. Then one measures a specimen using *Match Fingerprint*, and the built-in screen shows the closest matching reference in realtime. To identify a matching reference material, the algorithms use a Pearson's chi-squared (χ^2) test as a means to determine goodness of fit between the spectrum from a specimen and those in the library (Hejzlar and Pesce, 2009). This statistic is one of the most common metrics for "best fits" in spectrometry.

Specifically, the Niton software uses measured X-ray intensities from 24 pre-set elements to calculate the mean squared distance (MSD) between measurements from a specimen and each reference material within the library. If the spectra from a specimen and a reference material perfectly match, the MSD is zero. As differences increase, the MSD increases as well. As soon as one starts measuring a specimen, the LCD displays the name of the one or two best matches from the library and the MSD for each. Thus, calculated and displayed in realtime, is a statistical metric of the matches between a specimen and the reference population.

5.2. Limitations of the "Spectral Fingerprints" method

One weakness of this method is the pre-set list of 24 elements: Sb, Sn, Pd, Ag, Al, Mo, Nb, Zr, Bi, Re, Pb, Se, W, Ta, Zn, Hf, Cu, Ni, Co, Fe, Mn, Cr, V, and Ti. These elements allow identification of over 400 metal alloys, but many are not particularly useful for obsidian. Nb and Zr are very useful for obsidian sourcing. Ta and Hf, for example, can be useful for obsidian but occur at concentrations that require the sensitivity of NAA. Sr and Rb, however, are missing, and elements such as W and Ni are unlikely to yield much discriminating power. At present, elements cannot be added or removed to the *Spectral Fingerprint* mode (but this may change in the future). Nevertheless, we felt that this method was worth exploring due to the multitude of elements used to derive the fingerprints, following Harbottle's approach.

Another drawback is that X-ray intensities are not converted into element concentrations. Measurements are reported in cps/μA (i.e., X-ray counts per second per microAmp of X-ray tube current) rather than parts per million (ppm) or weight percent. This simplifies the algorithms for realtime χ^2 calculations against potentially hundreds of reference materials. Because the *Spectral Fingerprint* mode is comparative, only measured X-ray intensities are recorded, and no matrix or overlap corrections are made to the measurements. Nevertheless, this method is quantitative because all X-ray intensities for the references and specimens are recorded, statistically matched, and available as a spreadsheet for documentation or further statistical testing. Measuring and reporting X-ray intensities was once standard (e.g., Ambrose et al., 1981; Brown, 1983; Godfrey-Smith and Haywood, 1984; Shackley, 1988), and most of the foundational obsidian studies are based on intensities (e.g., Jack and Heizer, 1968; Jack and Carmichael, 1969). Today, however, reporting X-ray intensities is commonly considered insufficient (e.g., Shackley, 2005), but while uncommon, it is not unheard of (e.g., Astruc et al., 2007).

We concur that, if possible, geochemical measurements of artifacts and specimens should be fully quantitative and generally compatible with data collected by archaeometric laboratories. As noted in Section 4.2, all artifacts and geological specimens were previously analyzed using fully calibrated pXRF. For our specialized applications, however, we are willing to consider a method based on X-ray intensities rather than elemental data, and as noted in Section 3.2, there already are distinct technique-based communities of practice in obsidian sourcing. Thus, while we are interested in the long-term utility of our raw data, our primary goal is producing correct source identifications useful to our team during excavations and surveys.

Lastly, metal identification commonly involves flat surfaces and, for alloys like stainless steel, minimal surface alteration. It was unknown at the outset of this study how the curvature and weathering of artifacts would affect our results. Using ceramics, pXRF tests by Forster et al. (2011) demonstrate that elements are not equally affected by surface effects. Light elements, like Si, Ca, and Ti, are strongly affected by convex, concave, and grooved surfaces, whereas heavy elements like Rb, Sr, and Zr are largely immune. The same trend was reported for surface coatings. Therefore, if suitable elements dominate the fingerprint in *Spectral Fingerprint* mode, the results could be largely unaffected by surface irregularities.

5.3. "Teach Fingerprints" protocols

The instrument was "taught" twelve obsidian spectra for this test (Fig. 1): Pokr Arteni, Mets Arteni, Gutansar, Hatis, Geghasar, Syunik-1 (Pokr and Mets Sevkar), Syunik-2 (Mets Satanakar and Bazenk), Tsakhkunyats-1 (Arkayasar/Kamakar), Tsakhkunyats-2 (Ttvakar), and Tsakhkunyats-3 (Damlik). Each type was represented by one polished specimen characterized by NAA, XRF, and EMPA. Although the software has the capability to store hundreds of fingerprints, we used one specimen per obsidian type for two reasons. The first was speed. Obsidian sources are, with few exceptions, geochemically homogeneous (e.g., Glascock et al., 1998: 18, Hughes, 1998: 107, Shackley, 2008: 198), and with one specimen each, we taught the software all twelve obsidians in less than 20 min. We could pick up a new instrument and use this method in minutes. Second, the software reports only the two best matches, so using two or more specimens would mean not knowing the second-best match.

When the fingerprints are plotted (Fig. 3), our data suggest that most elements provide a degree of discrimination. This might be due partly to the uncorrected nature of these data (i.e., they are unadjusted for interferences from other elements). This is sometimes due to an element already in the fingerprint. For example, Co appears to vary considerably, but the measurements likely reflect interferences from Fe X-rays. In contrast, the Bi data likely include

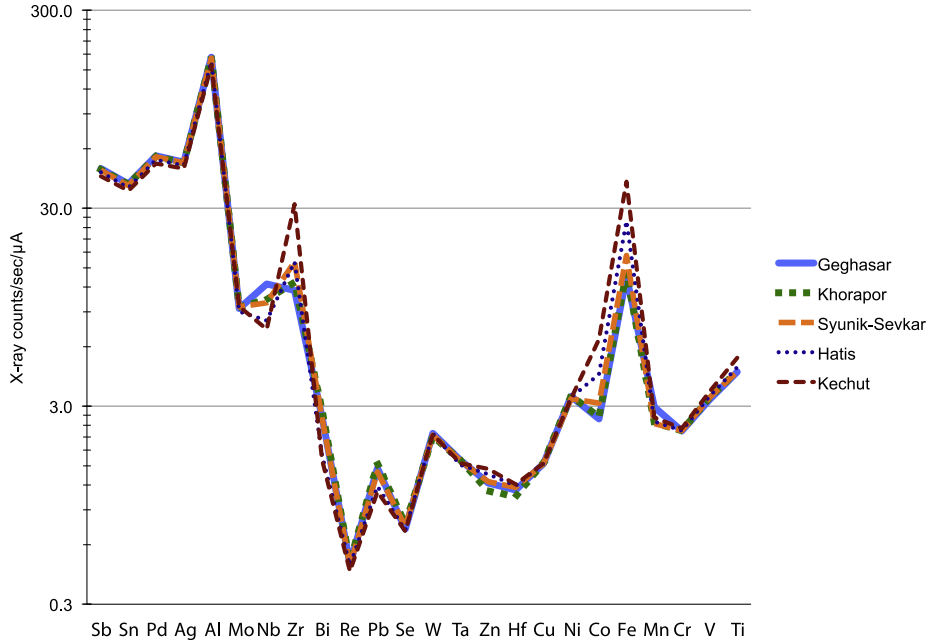

Fig. 3. Comparison of "spectral fingerprints" for different obsidian sources. Only five are shown here for clarity. The vertical axis is the X-ray intensity for each element, measured in X-ray counts per second per microAmp of X-ray tube current and plotted on a logarithmic scale.

interferences from Ba, an element useful in obsidian sourcing. Thus, fingerprints include subtle contributions from elements beyond the pre-set list, and such interferences become fortuitous (e.g., Ba is not included in the pre-set list of elements, but it nevertheless contributes to the overall fingerprint due to its uncorrected contributions to the Bi X-ray intensity measurements).

5.4. Testing protocols for geological specimens and artifacts

First, 485 geological specimens were analyzed once for 10 s. Of these specimens, 459 corresponded to the twelve Armenian obsidians for which the software had fingerprints in its reference library, and 26 came from Georgia and Turkey. All specimens were analyzed on unprepared surfaces, which varied from smooth flake scars to weathered exteriors. This test used a cardboard stand, designed to be lightweight and duplicated anywhere in the world.

Second, the 154 artifacts were measured for 10 s, and the instrument was used as it would be in the field. Operation was entirely handheld without a laptop, electricity, or test stand. Analyses were started by the trigger and ended automatically after 10 s. Positioning was aided by the instrument's internal camera. The artifact surface selected for analysis was simply the one considered least likely to puncture a film over the measurement window. Analyses were conducted outdoors in conditions that varied from direct sunlight to light rain.

5.5. Results for geological specimens and artifacts

Fig. 4 demonstrates what the pXRF displays. For Gutansar and Hatis, the match was sufficiently definitive that only the best fit and its χ^2 value were displayed. For the Pokr Arteni specimen, the correct source is marginally better than the B-ranked Mets Arteni. For a Syunik-Sevkar specimen, Syunik-Satanakar is a close second-best fit. The Tsakhkunyats-2 specimen is correctly identified, and Tsakhkunyats-3 is ranked as the next-best match.

Table 3 summarizes the A- and B-rank matches and their χ^2 values for the 459 Armenian geological specimens, and Supplementary Table S1 gives specimen-by-specimen results. Only seven were misidentified. Five specimens from Mets Arteni were matched to Pokr Arteni, just 3 km away (with Mets Arteni as close B-rank matches). A Syunik-Sevkar specimen was matched to Syunik-Satanakar, and vice versa. For both, the χ^2 values were virtually identical.

To establish how the software would handle obsidians not in the library, we analyzed 26 specimens from Georgia and Turkey. Table 4 summarizes the A- and B-rank matches and their χ^2 values for these specimens, and Supplementary Table S2 gives specimen-by-specimen results. The Nemrut Dağ specimen yielded χ^2 values so high that the screen displayed "No Match," and the Bingöl B specimens had χ^2 values above 1, indicating poor matches. The other nine Turkey specimens had χ^2 values between 0.43 and 0.92, and their A- and B-rank matches are anomalous compared to Table 3. For example, the Sarıkamış specimen had an A-rank match of Syunik-Sevkar, but the B-rank was Pokr Arteni, not Syunik-Satanakar. Hence, A- and B-rank matches that make little geochemical sense can suggest a mismatch. Georgian specimens were matched to Tsakhkunyats-3 and Hatis, not Chikiani, and their χ^2 values may be too small to be recognized as erroneous. Therefore, we propose including a Chikiani fingerprint in future work.

Table 5 summarizes the A- and B-rank matches and their χ^2 values for the 154 artifacts, and Supplementary Table S3 lists artifact-by-artifact results. Generally the artifacts have higher χ^2 values than the geological specimens. This is likely due to a combination of artifacts' uneven, weathered surfaces (i.e., hydration on a sub-millimeter scale) and handheld operation adding small geometric errors (i.e., less-than-ideal geometric alignments of X-ray tube, artifact, and detector). Nevertheless, all 154 artifacts were correctly matched to their sources.

6. Method 2: discriminant functions with pass/fail mode

Our second method uses two software features: (1) "pass/fail" mode for testing consumer products and (2) "pseudo-elements," commonly used to automatically calculate percent oxide or

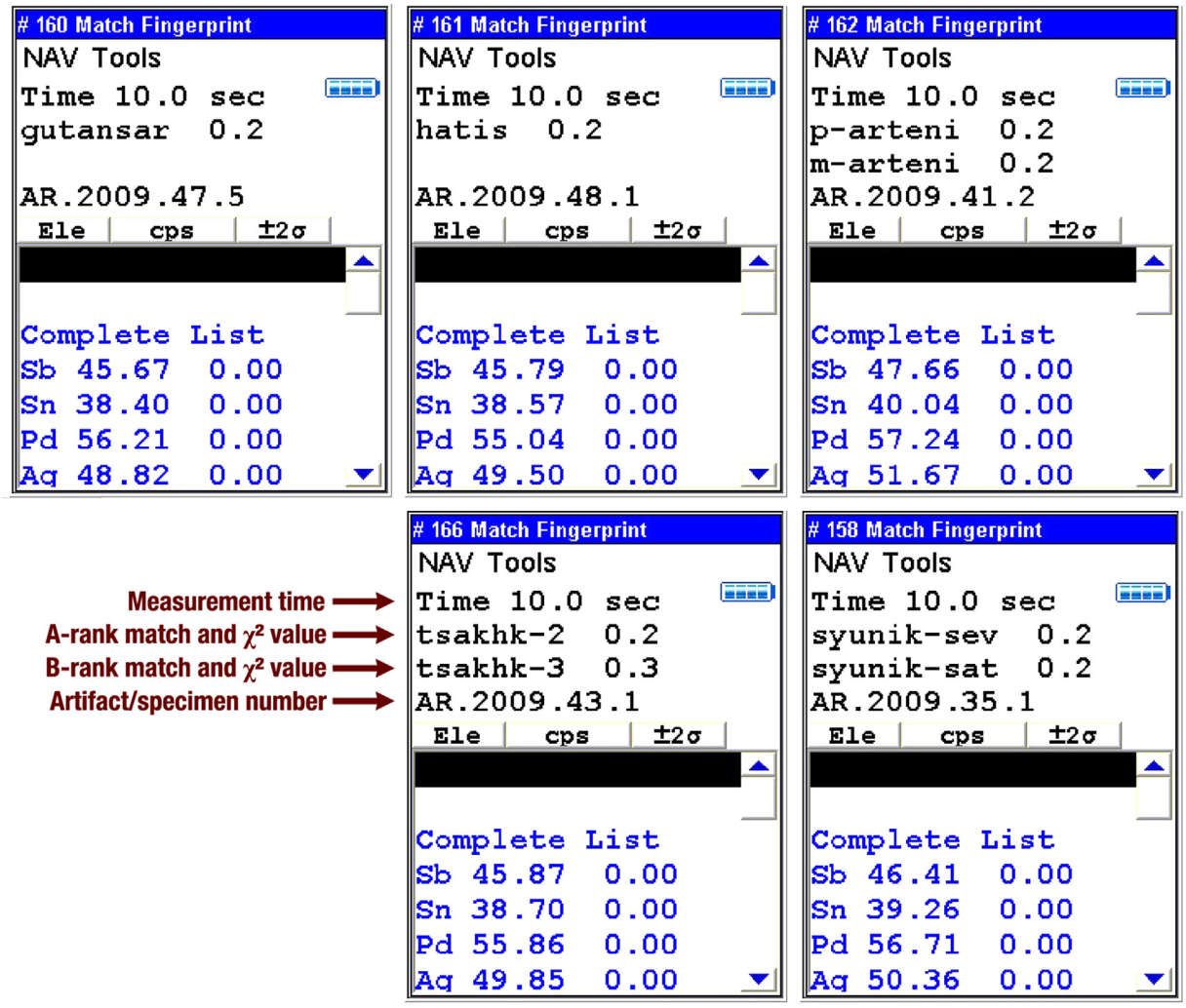

Fig. 4. These screen captures of the pXRF instrument's built screen demonstrate how the best matching sources (and their "goodness of fit" based on χ^2 values) are displayed to a user after 10 s using the *Spectral Fingerprints* method.

element ratios. This method follows Hughes' approach to classification, and it remedies the key weakness of our first method: a lack of quantitative elemental data.

6.1. Using the pass/fail and pseudo-element algorithms

pXRF is often used to test consumer products for compliance with regulatory limits. For example, the software can be used with pass/fail criteria for the European Union's Restriction of Hazardous Substances Directive (RoHS). RoHS prohibits, for example, Pb above 1000 ppm. A Pb concentration over 1300 ppm results in the measurement highlighted in red to mark a "fail." If Pb is below 700 ppm, the result is a green "pass." A yellow "inconclusive" results if the level falls in the intermediate range. Thresholds may be set for any element; however, the algorithms are rather simple. The software assumes "pass" is below a low threshold and "fail" is above a high one. There is no way to define an intermediate range as "pass."

Another issue is illustrated by Fig. 5. Suppose one wishes to distinguish two obsidians based on Elements A and B. Neither source can be defined by ranges of Elements A and B due to overlaps. There is, though, an axis on which the two populations are perfectly differentiated: line *c-d*. This axis combines Elements A and B in a discriminant function (line *e-f*). With more elements, discriminant analysis (DA) derives the best discriminating axes in higher dimensions. These functions can also classify new observations (i.e., analyzed artifacts).

The general form of a discriminant function is:

$$D = c_1X_1 + c_2X_2 + c_3X_3 + \ldots + c_iX_i + A$$

where D = discriminant function; c = discriminant coefficients; X = original variables (e.g., elements); i = number of variables; A = constant.

Such an equation is compatible with the software's "pseudo-elements." For example, a geologist may be more interested in the ratio of CuO to NiO in a rock outcrop than the absolute Cu and Ni contents. The software can report a pseudo-element defined as (Cu × 1.252)/(Ni × 1.273), and the calculations are done automatically and displayed onscreen. If that geologist is interested in identifying rocks above a particular ratio, pass/fail thresholds could be defined (and quantitative data for Cu and Ni would still be acquired to calculate the pseudo-element).

Consequently, we derived discriminant functions, entered them as pseudo-elements, and calculated thresholds for six Armenian obsidian source complexes. It must be emphasized that, to calculate the pseudo-elements, fully quantitative elemental data (i.e., data

Table 3
Summary of the A- and B-rank matches for 459 Armenian geological obsidian specimens with "fingerprints" in the custom reference library and their χ^2 values based on the *Spectral Fingerprint* method. Erroneous identifications are italicized. See Supplementary Table S1 for specimen-by-specimen results.

Complex	Source	*n*	A-rank matches				B-rank matches			
			Fingerprint	*n*	%	Mean χ^2	Fingerprint	*n*	%	Mean χ^2
Gutansar	–	240	gutansar	240	100%	0.27	hatis	220	92%	0.58
							tsakhk-2	14	6%	0.63
							kechut	4	2%	0.83
							tsakhk-1	2	1%	0.73
Hatis	–	87	hatis	87	100%	0.28	tsakhk-3	81	93%	0.33
							tsakhk-2	5	6%	0.41
							gutansar	1	1%	0.39
Arteni	Pokr Arteni	54	p-arteni	54	100%	0.26	m-arteni	53	98%	0.31
							syunik-sev	1	2%	0.39
	Mets Arteni	43	m-arteni	38	88%	0.25	p-arteni	38	88%	0.27
			p-arteni	*5*	*12%*	*0.24*	*m-arteni*	*5*	*12%*	*0.25*
Tsakhkunyats	Tsakhkunyats-1	2	tsakhk-1	2	100%	0.25	tsakhk-2	2	100%	0.43
	Tsakhkunyats-2	4	tsakhk-2	4	100%	0.25	tsakhk-3	4	100%	0.29
	Tsakhkunyats-3	4	tsakhk-3	4	100%	0.30	tsakhk-2	3	75%	0.30
							hatis	1	25%	0.50
Syunik	Mets and Pokr Sevkar	6	syunik-sev	5	83%	0.22	syunik-sat	5	83%	0.24
			syunik-sat	*1*	*17%*	*0.24*	*syunik-sev*	*1*	*17%*	*0.25*
	Mets Satanakar, Bazenk	7	syunik-sat	6	86%	0.25	syunik-sev	3	43%	0.25
							chorapor	3	43%	0.27
			syunik-sev	*1*	*14%*	*0.40*	*syunik-sat*	*1*	*14%*	*0.40*
Geghasar	Geghasar-1	6	geghasar	6	100%	0.24	chorapor	6	100%	0.26
	Spitakasar	1	geghasar	1	100%	0.24	chorapor	1	100%	0.25
Khorapor	–	1	choraphor	1	100%	0.22	geghasar	1	100%	0.26
Kechut	Aghvorik	4	kechut	4	100%	0.26	gutansar	4	100%	1.08

corrected for matrix effects, calibrated, and converted into element concentrations) are acquired simultaneously.

6.2. Selecting elements for discriminant analysis

Five elements were selected for DA: Zr, Sr, Rb, Nb, and Fe. For two reasons, these are among the elements most frequently used for obsidian sourcing (e.g., Seelenfreund et al., 2002; Silliman, 2005; Negash and Shackley, 2006; Carter and Shackley, 2007; De Francesco et al., 2008; Phillips and Speakman, 2009; Shackley, 2009). First, their concentrations vary little within obsidian flows but can vary as much as three orders of magnitude among volcanoes (Rapp and Hill, 2006:225). Second, due to X-ray physics, elements in "mid-Z" portion of the periodic table are measured especially well with XRF (e.g., Giaque et al., 1993). Shackley (2008) notes these elements are "some of the most sensitive" for sourcing (203). Therefore, this method follows a Hughesian approach: using the best-measured, most-discriminating elements.

These elements are also measured using the "main" X-ray filter and, therefore, can be simultaneously quantified. Other elements, including Ba and Ti, have proven useful in prior obsidian sourcing studies. However, Ba must be measured using Niton's "high" filter, which would increase the measurement duration. Similarly, Ti can be detected using the main filter; however, precise quantification at its concentrations in obsidian requires the "low" filter.

As noted in Section 4.1, measurement uncertainty is inversely proportional to the square root of the measurement time. Fig. 6 shows the results of our tests regarding this relationship for Zr, Sr, Rb, Nb, and Fe. For all five elements, uncertainties are below 10% (at the 2σ-level) after 10 s. In fact, for Sr and Rb, the uncertainty is 6% after 10 s, and for Zr and Fe, it is 4%. Consider that NAA has uncertainties of 2–5% for elements such as Rb and 5–10% for Sr and Zr (Glascock et al., 2007: 346). After 10 s, these elements have uncertainties comparable to NAA data, and there is little point in longer measurements.

6.3. Weaknesses of DA with pseudo-elements

With a limit of 15 pseudo-elements, defining populations using two to three discriminant functions restricted us to five to seven

Table 4
Summary of the A- and B-rank matches for 26 geological obsidian specimens without "fingerprints" in the custom library and their χ^2 values based on the *Spectral Fingerprint* method. See Supplementary Table S2 for specimen-by-specimen results.

Region	Source	*n*	A-rank matches				B-rank matches			
			Fingerprint	*n*	%	Mean χ^2	Fingerprint	*n*	%	Mean χ^2
Turkey	Nemrut Dağ	1	kechut	1	100%	56.64	gutansar	1	100%	68.43
	Bingöl B	2	kechut	2	100%	1.10	gutansar	2	100%	1.78
	Muş	1	gutansar	1	100%	0.86	syunik-sev	1	100%	1.59
	Meydan Dağ	4	gutansar	4	100%	0.82	kechut	4	100%	1.40
	Tendürek Dağ	2	gutansar	2	100%	0.92	kechut	2	100%	1.54
	Süphan Dağ	1	hatis	1	100%	0.63	gutansar	1	100%	0.63
	Sarıkamış	1	syunik-sev	1	100%	0.43	p-arteni	1	100%	0.46
Georgia	Chikiani	14	tsakhk-3	9	64%	0.37	hatis	7	50%	0.48
							p-arteni	2	14%	0.47
			hatis	5	36%	0.33	tsakhk-3	4	29%	0.37
							p-arteni	1	7%	0.45

Table 5
Summary of the A- and B-rank matches for 154 Palaeolithic obsidian artifacts and their χ^2 values based on the *Spectral Fingerprint* method. See Supplementary Table S3 for artifact-by-artifact results.

Complex	Source	*n*	A-rank matches				B-rank matches			
			Fingerprint	*n*	%	Mean χ^2	Fingerprint	*n*	%	Mean χ^2
Arteni	Pokr Arteni	1	p-arteni	1	100%	0.37	m-arteni	1	100%	0.43
Gutansar	–	149	gutansar	149	100%	0.31	hatis	130	87%	0.64
							kechut	13	9%	0.81
							tsakhk-2	5	3%	0.62
							tsakhk-1	1	1%	0.74
Hatis	–	1	hatis	1	100%	0.29	tsakhk-3	1	100%	0.37
Syunik	Mets and Pokr Sevkar	1	syunik-sev	1	100%	0.31	syunik-sat	1	100%	0.35
Tsakhkunyats	Arkayasar/Kamakar	1	tsakhk-1	1	100%	0.30	tsakhk-2	1	100%	0.39
	Damlik	1	tsakhk-3	1	100%	0.26	tsakhk-2	1	100%	0.29

groups. Using the XLSTAT Pro statistical package, we derived three discriminant functions based on more than 1800 analyses from six obsidian source complexes (Fig. 1): Arteni ($n = 356$), Geghasar ($n = 58$), Gutansar ($n = 886$), Hatis ($n = 330$), Syunik ($n = 81$), and Tsakhkunyats ($n = 78$). Therefore, as a trade-off for fully quantitative elemental data, the distinction between, for example, Pokr and Mets Arteni obsidians would not be evident in the field with this configuration, but subsequent data analyses could discern them. If distinguishing Pokr and Mets Arteni was important, newly derived functions could do so.

6.4. Using discriminant functions

We derived three discriminant functions using Nb, Zr, Sr, Rb, and Fe, and since pseudo-elements are assumed to yield positive numbers, the functions' constants were increased so that all results are positive. The final equations are:

$$F1 = 2.36 \times Nb + 2.07 \times Zr - 2.86 \times Sr + 0.064 \times Rb + 0.011 \times Fe + 80$$

$$F2 = 2.42 \times Nb + 0.43 \times Zr + 0.39 \times Sr + 0.032 \times Rb + 0.007 \times Fe - 80$$

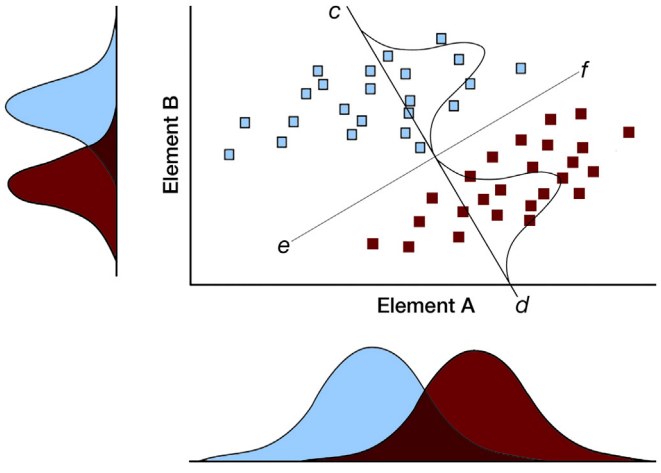

Fig. 5. Simplified example of two obsidian sources and their concentrations of Elements A and B. Neither source can be defined by ranges of Elements A and B due to overlaps. There is, though, an axis on which the two populations are perfectly differentiated: line *c*–*d*. This new axis combines Elements A and B in a single discriminant function (line *e*–*f*).

$$F3 = -5.82 \times Nb - 0.30 \times Zr - 0.15 \times Sr + 2.51 \times Rb + 0.016 \times Fe + 30$$

The first two functions account for 94.6% of the variability in the dataset, and all three functions account for 98.3% of the variability. Fig. 7 shows the transformation of our elemental data to maximize separation among the six source complexes and how the five elements contribute to each function. Based on our *a priori* knowledge of Armenian obsidians, these functions can be used to assign newly analyzed artifacts to their most likely sources.

Each complex was defined by the first two or all three functions as pseudo-elements, and thresholds were based on our 1800 analyses of Armenian geological obsidian specimens (Table 6). The functions were identical for all six complexes; only the thresholds differed, derived from the maximum and minimum values for the geological specimens. An alternative approach could use distinct functions for every complex, and each set of functions could be specially derived to maximize the differences between one particular complex and all others.

Each series of thresholds defined the "intermediate" range for each complex. When the value for a discriminant function (as a pseudo-element) falls in the range for a particular source complex, that value turns yellow onscreen, corresponding to the "intermediate" range in pass/fail mode. Too low a value is green; too high is red. When the two or three functions that define a complex all display yellow values onscreen, it is a match. Fig. 8 shows examples. Gutansar, Hatis, and Tsakhkunyats are each defined by two functions, and when both of their respective functions display yellow values, it is a match. Arteni and Syunik are defined by all three functions, and a match occurs when all three display yellow values.

6.5. Testing protocols for geological specimens and artifacts

First, 499 geological specimens were analyzed three times each for 10 s: 467 from the six obsidian source complexes included the DA and 31 from Georgia, Turkey, and Armenian sources excluded from the DA. Analyses were conducted in the "mining" mode, which uses FP correction to adjust measurements for X-ray emission, absorption, and other phenomena. The conditions were otherwise the same as the first method. Second, the 154 artifacts were measured for 10 s. Again the analyzer was operated in handheld mode, and weather conditions varied from direct sunlight to light rain.

6.6. Results for the geological specimens and artifacts

Table 7 summarizes the matches for the 467 specimens from the six source complexes, and Supplementary Table S4 gives analysis-by-analysis results. Of the 1391 analyses, only one analysis of a

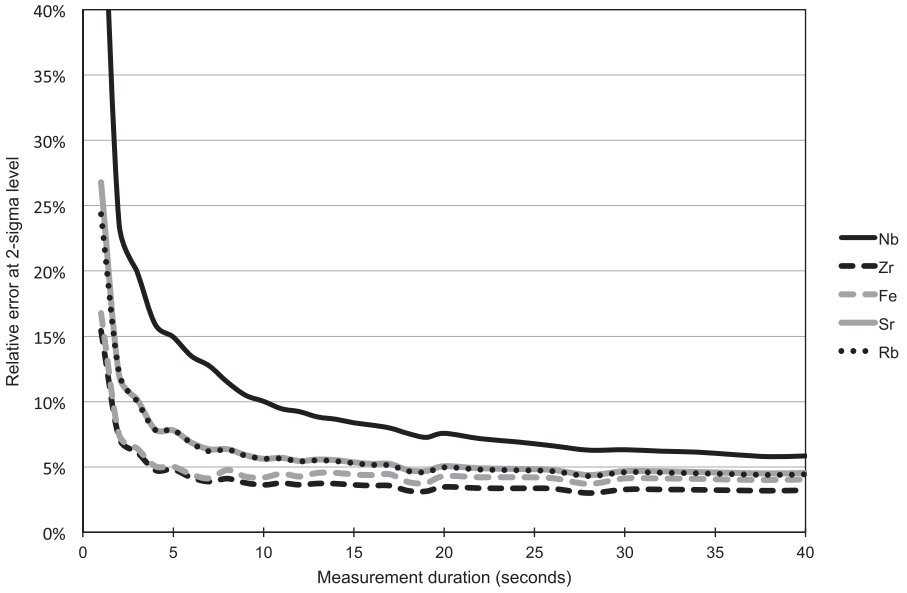

Fig. 6. Our tests show the inverse square relationship between measurement uncertainty and time for Zr, Sr, Rb, Nb, and Fe for a Gutansar obsidian specimen. The specimen was measured multiple times for a series of durations between 1 and 40 s. After 10 s, these five elements have measurement uncertainties comparable to NAA data.

Gutansar specimen yielded no match, but its quantitative elemental data (collected simultaneously) could still be readily matched to the proper volcano. All other analyses match the correct volcanic complex.

We analyzed 31 specimens to determine what happens when "unknown" specimens are encountered. Table 8 summarizes the findings for these specimens, and Supplementary Table S5 reports analysis-by-analysis results. All ten specimens from

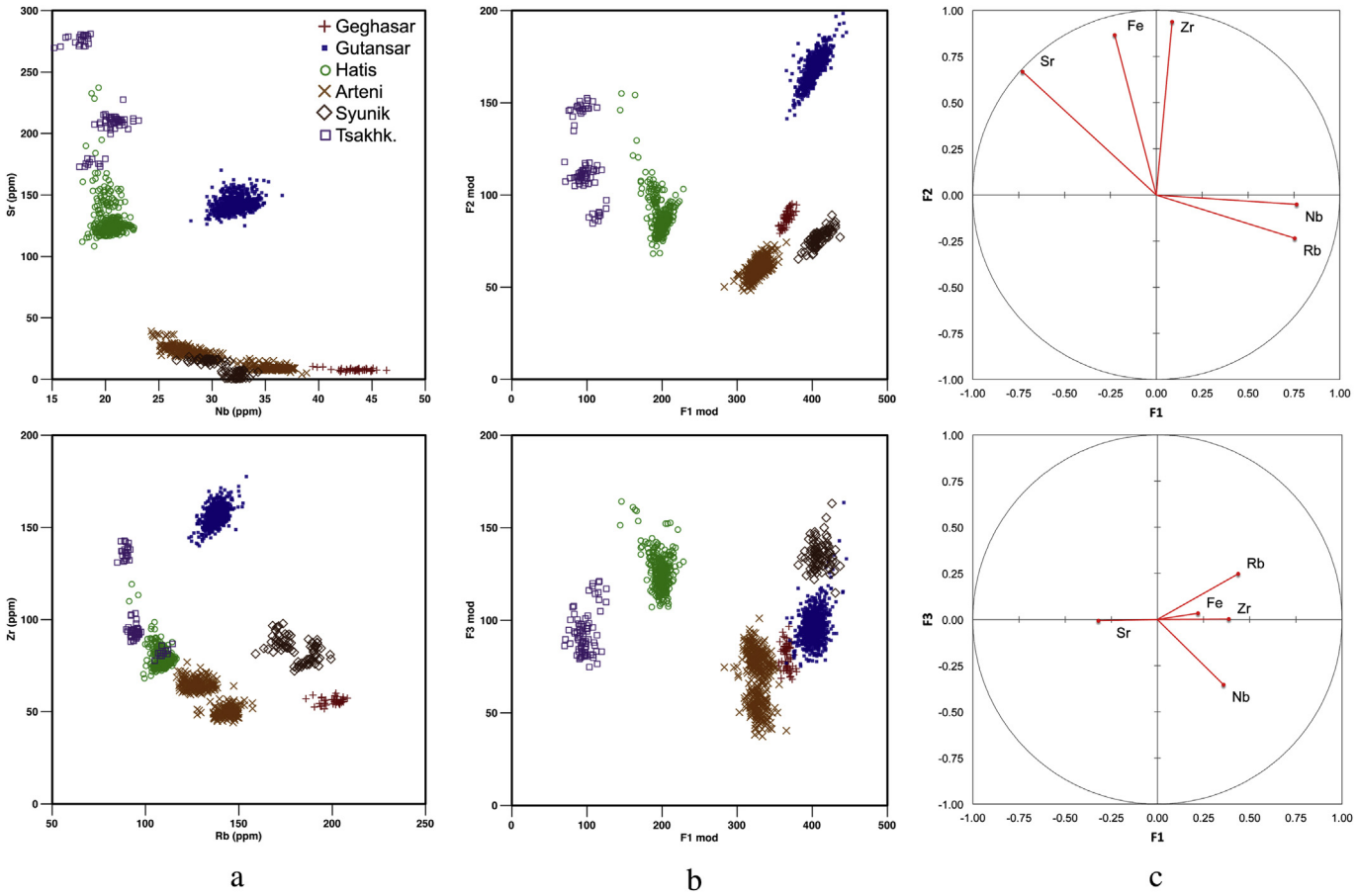

Fig. 7. The transformation of our elemental data (a) using discriminant analysis to maximize the separation among the six Armenian source complexes (b) and how the five elements contribute to each of the three discriminant function (c).

Table 6
Pass/intermediate/fail thresholds for the discriminant functions for the six Armenian source complexes. "Actual" denotes the empirically derived boundaries for each function and complex based on more than 1800 analyses of geological specimens using conventional pXRF methods. "Threshold" denotes the values used in the pXRF software and subsequently tested with 10-s analyses of geological specimens and Palaeolithic artifacts.

		F1		F2		F3	
		Actual	Threshold	Actual	Threshold	Actual	Threshold
Arteni	Max (Fail)	366	370	74	80	101	110
	Min (Pass)	283	270	48	30	37	30
Geghasar	Max (Fail)	379	390	95	100	97	110
	Min (Pass)	355	340	79	70	68	60
Gutansar	Max (Fail)	445	460	198	200	–	–
	Min (Pass)	365	350	141	130	–	–
Hatis	Max (Fail)	228	230	155	170	–	–
	Min (Pass)	143	130	69	60	–	–
Syunik	Max (Fail)	437	450	89	100	163	170
	Min (Pass)	382	370	65	40	115	110
Tsakhkunyats	Max (Fail)	125	130	153	160	–	–
	Min (Pass)	69	50	85	80	–	–

Turkey had no match. For the Georgian obsidian, 40 of 42 analyses had no match, and two analyses matched Hatis (and other analyses for these specimens had no match). One specimen from Khorapor was matched to the Syunik complex. Khorapor is geographically and geochemically close to Syunik, so the result is neither unexpected nor detrimental. Khorapor obsidian is chemically distinguishable from the Syunik sources, so refinements to or rederivations of the

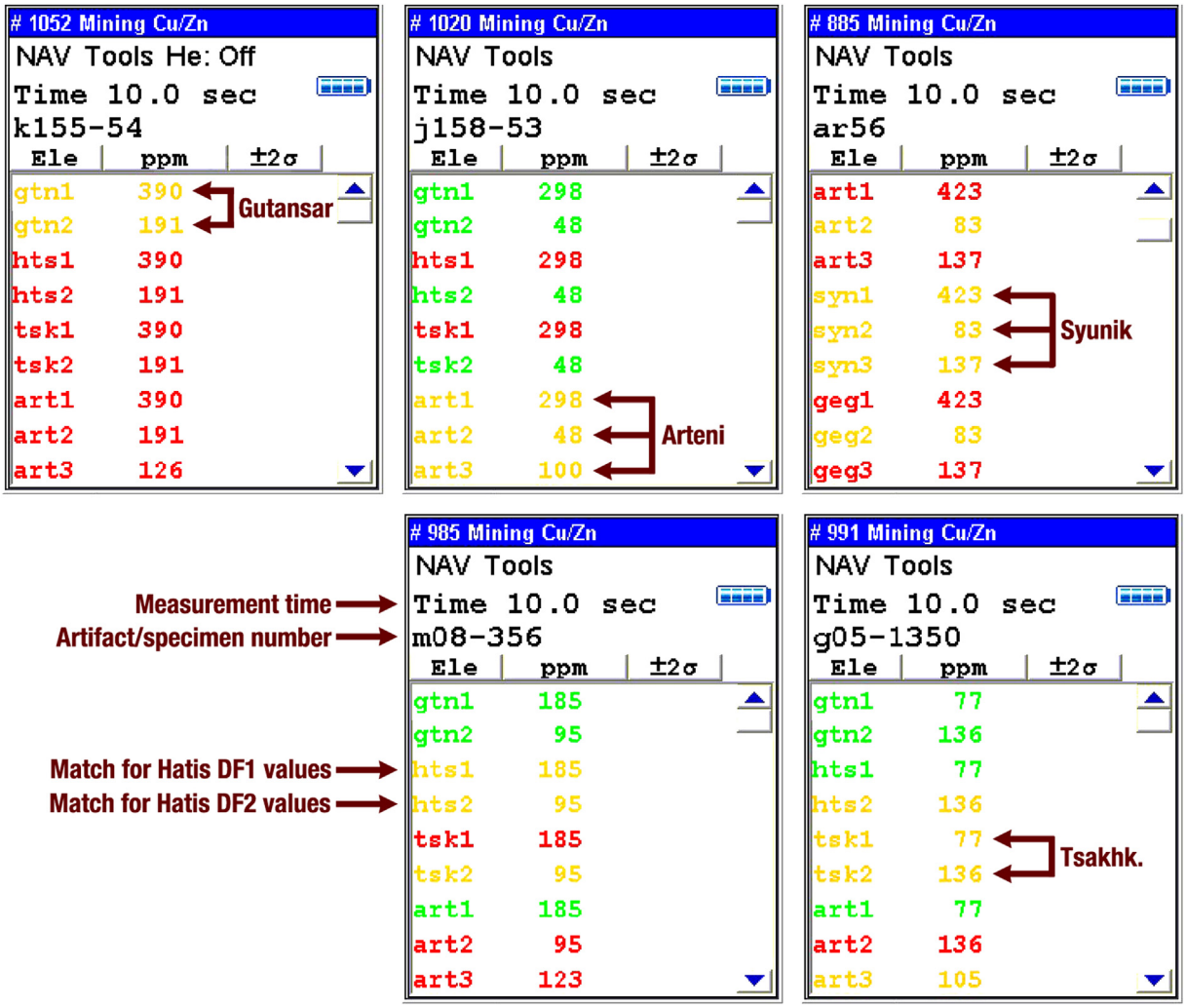

Fig. 8. These screen captures of the pXRF instrument's built screen demonstrate how a matching source is displayed to a user after 10 s using the discriminant analysis method. Gutansar, Hatis, and Tsakhkunyats are each defined by two discriminant functions, and when both of their respective functions display yellow values, it is a match. Arteni and Syunik are defined by all three functions, and a match occurs when all three display yellow values.

Table 7
Summary of the matches for 467 Armenian geological obsidian specimens included in our discriminant analysis. One erroneous identification is italicized. See Supplementary Table S4 for analysis-by-analysis results.

Complex	Source	Specimens	Analyses	Match	Analyses	%
Arteni	Metz Arteni	43	129	Arteni	129	100%
	Pokr Arteni	54	162	Arteni	162	100%
Gegham	Geghasar	9	17	Geghasar	27	100%
Gutansar	–	249	747	Gutansar	746	99.9%
				No match	*1*	*0.1%*
Hatis	–	89	267	Hatis	267	100%
Syunik	Syunik-1: Sevkar (Mets and Pokr Sevkar)	7	21	Syunik	21	100%
	Syunik-2 (Mets Satanakar and Bazenk)	8	24	Syunik	24	100%
Tsakhkunyats	Tsakhkunyats-1 (Arkayasar/Kamakar)	2	6	Tsakhkunyats	6	100%
	Tsakhkunyats-2 (Ttvakar)	4	12	Tsakhkunyats	12	100%
	Tsakhkunyats-3 (Damlik)	2	6	Tsakhkunyats	12	100%

discriminant functions may reduce or eliminate this misidentification in the future.

A problem is that two Spitakasar specimens were matched to the Arteni complex. These obsidians are also similar chemically, so the overlap is unsurprising. It is unclear whether this result is archaeologically troublesome. Our team identified no Spitakasar artifacts, and recent studies of Armenian obsidians (e.g. Badalyan et al., 2004; Chataigner and Gratuze, 2013a,b) analyzed no Spitakasar obsidian. We anticipate that discriminant functions could be rederived, perhaps including additional elements (cf. data in Keller et al., 1996), to account for Spitakasar obsidian and reduce or eliminate the overlap with the Arteni complex.

Table 9 summarizes the matches for the 154 Armenian artifacts, and Supplementary Table S6 gives artifact-by-artifact results. All but two artifacts had matches, and all 152 matches were correct. Two Gutansar artifacts yielded no match, but their quantitative elemental data (collected simultaneously) would still be readily attributed to the proper volcano.

7. Discussion and conclusions

Here we demonstrate two methods of sourcing obsidian artifacts in just 10 s while in the field. A claim of automated, on-site source identification in only seconds may be met with skepticism; however, through tests of both geological specimens and archaeological artifacts, we have established the validity and reliability of both methods. The technological ability to source obsidian artifacts rapidly on-site clearly exists, but the methods to do so effectively were hitherto undeveloped. The methods perform so well that there is no clear reason to recommend one over the other. For a particular application, a preference for either quantitative chemical data or more exact source identification will determine which one to use. Ultimately, both methods are so fast that they could be used together for a combined approach at a site or on a survey. For example, at a site where Gutansar obsidian dominates, exotics can be initially identified using the *Spectral Fingerprint* method and immediately reanalyzed using the DA method.

Two points are worth stressing. First, our methods are not intended to replace traditional sourcing procedures in the field house (using pXRF) or laboratory (using stationary instruments). Rather, they are intended to offer information previously unavailable in the field and to optimize resources (e.g., time, money) in subsequent sourcing efforts. Second, our methods have been developed only after considerable foundational research, including surveys and sampling of obsidian sources, source characterization by multiple techniques, and analyses of more than 500 geological specimens and 1700 archeological artifacts. As such, our approach critically depends on, rather than undermines, conventional obsidian sourcing procedures.

The situation is analogous to that regarding the different approaches to obsidian sourcing with EMPA. To precisely analyze numerous elements in obsidian source specimens, researchers have used measurement durations of a few minutes (e.g., Tykot, 1995; Weisler and Clague, 1998; Frahm, 2012). Merrick and Brown (1984), however, were interested in rapid sourcing of Kenyan obsidian artifacts. After characterizing geological specimens using XRF and wet chemistry, they identified three elements able to discern most sources: Ca, Ti, and Fe. With additional analytical choices made to optimize for speed, each artifact was measured for 10–12 s. If Merrick and Brown (1984), using a 1960s-vintage electron microprobe, were able to acquire sufficiently precise measurements in 10 s for obsidian sourcing, it should be unsurprising that a state-of-the-art pXRF analyzer could do the same. As recently pointed out by Speakman and Shackley (2013), the newest generation of pXRF instruments has better detectors and electronics than lab-based XRF systems manufactured just five years ago.

Regarding chert sourcing, Luedtke (1992) argued that a "good source analysis is usually complex and expensive, and should not be initiated merely as a fishing expedition in the vague hope that you might find something interesting" (117). Our approach to on-site

Table 8
Summary of the matches (or lack thereof) for 31 geological obsidian specimens excluded from our discriminant analysis. The erroneous identifications are italicized. See Supplementary Table S5 for analysis-by-analysis results.

Region	Complex	Source	Specimens	Analyses	Match	Analyses	%
Armenia	Khorapor	–	1	3	*Syunik*	*3*	*100%*
	Gegham	Spitakasar	2	6	*Arteni*	*12*	*100%*
	Kechut	Aghvorik	4	12	No match	12	100%
Georgia	Chikiani	–	14	42	No match	40	95%
					Hatis	*2*	*5%*
Turkey	Kars	Arpaçay	1	3	No match	3	100%
	Meydan Dağ	–	5	15	No match	15	100%
	Tendürek Dağ	–	3	9	No match	9	100%
	Sarıkamış	–	1	3	No match	3	100%

Table 9
Summary of the matches for 154 Palaeolithic artifacts using the discriminant analysis method. See Supplementary Table S6 for artifact-by-artifact results.

Complex	*Source*	*n*	*Match*	*n*	*%*
Arteni	Pokr Arteni	1	Arteni	1	100%
Gutansar	–	149	Gutansar	147	99%
			No match	*2*	*1%*
Hatis	–	1	Hatis	1	100%
Syunik	Syunik-1: Sevkar (Mets and Pokr Sevkar)	1	Syunik	1	100%
Tsakhkunyats	Tsakhkunyats-1 (Arkayasar/ Kamakar)	1	Tsakhkunyats	1	100%
	Tsakhkunyats-3 (Damlik)	1	Tsakhkunyats	1	100%

sourcing might be seen, at least by some, as a fishing expedition. We would reply to such a view in two ways. First, the research here is based on our *a priori* knowledge of Armenian obsidians, including the important obsidian sources at sites for which we have done sourcing and our initial exploration of spatiotemporal patterns in their use at those sites. Furthermore, our work in the field house to source artifacts excavated or collected on surveys just days earlier established the desirability of this information in the field. By the time volcanic sources were identified for recently recovered artifacts, excavations had proceeded, and a chance for any specialized sampling of the artifacts' contexts, if so desired, had passed. Additionally, by the time we had sourcing results for a few artifacts collected during a survey, our team had since moved on to a different area or site, providing no opportunity for feedback regarding, for example, possible occupation phases at the site. Second, because pXRF can source artifacts rapidly and inexpensively, we can commit less time and money to more targeted and speculative modes of inquiry. With reduced financial and time constraints, we should be more willing to pursue new approaches that, for example, employ obsidian sourcing to characterize sites at high spatial resolution.

By displacing obsidian sourcing from the context of "white lab coats" to that of "muddy boots," pXRF becomes a facilitating technology, removing physical (and temporal) barriers that have previously segregated archaeological practice between the field and the distant analytical laboratory (i.e., the traditional context of obsidian sourcing studies). The portability of handheld instruments can bring together field and laboratory practices in a common setting. Observations regarding obsidian artifacts, traditionally available only after the artifacts have been detached in both space and time from their archaeological contexts, can now be made in the field, providing almost immediate insights that can inform excavation and survey strategies.

Acknowledgments

The authors thank Pavel Avetisyan, Director of the Institute for Archaeology and Ethnography, Armenia, for his support of this project. We recognize the generous financial support for the Hrazdan Gorge Palaeolithic Project provided by the Norian Armenian Programs Committee (University of Connecticut, 2008–2013), a Large Faculty Grant (University of Connecticut, 2012), and the L.S.B. Leakey Foundation (2010 and 2011). Niton UK and Thermo Scientific are thanked for their insights and suggestions regarding spectral fingerprints and pseudo-elements. Additional Armenian obsidian specimens came from the Smithsonian Institution, specifically the collections of M. James Blackman and the late James F. Luhr. Obsidian specimens from Turkey were collected by George "Rip" Rapp, University of Minnesota and the late Tuncay Ercan, Directorate of Mineral Research and Exploration of Turkey. Georgian obsidian specimens came from Nino Sadradze and Givi Maisuradze, Institute of Geology, Georgian Academy of Sciences. Roger Doonan is thanked for his thoughts and insights on the topic at hand. Two anonymous reviewers made comments that led to clarifications of the final manuscript. This research was also supported by the Department of Archaeology at the University of Sheffield and the Marie Curie Network FP7-PEOPLE-2010-ITN: New Archaeological Research Network for Integrating Approaches to Ancient Material Studies (NARNIA).

Appendix A. Supplementary data

Supplementary data related to this article can be found online at http://dx.doi.org/10.1016/j.jas.2013.08.012.

References

Adler, D.S., Prindiville, T.P., Conard, N.J., 2003. Patterns of spatial organization and land use during the Eemian Interglacial in the Rhineland: new data from Wallertheim, Germany. Eurasian Prehist. 1 (2), 25–78.
Adler, D.S., Yeritsyan, B., Wilkinson, K., Pinhasi, R., Bar-Oz, G., Nahapetyan, S., Bailey, R., Schmidt, B.A., Glauberman, P., Wales, N., Gasparian, B., 2012. The Hrazdan Gorge Palaeolithic Project, 2008–2009. In: Avetisyan, P., Bobokhyan, A. (Eds.), Archaeology of Armenia in Regional Context, Proceedings of the International Conference Dedicated to the 50th Anniversary of the Institute of Archaeology and Ethnography Held on September 15–17, 2009 in Yerevan, Armenia. NAS RA Gitutyn Publishing House, Yerevan, pp. 21–37.
Ambrose, W.R., Duerden, P., Bird, J., 1981. An archaeological application of PIXE-PIGME analysis to Admiralty Islands obsidians. Nucl. Instrum. Methods 191, 397–402.
Astruc, L., Gratuze, B., Pelegrin, J., Akkermans, P., 2007. From Production to Use: a Parcel of Obsidian Bladelets at Sabi Abyad II. In: La diversité des systèmes techniques des communautés du Néolithique pré-céramique: vers la caractérisation des comportements sociaux. 5e colloque international sur les industries lithiques du Néolithique pré-céramique sous la direction de Laurence Astruc. Didier Binder et François Briois Éditions APDCA, Antibes, pp. 1–15.
Badalian, R., Bigazzi, G., Cauvin, M.-C., Chataigner, C., Bashyan Jr., R., Karapetyan, S., Oddone, M., Poidevin, J., 2001. An international research project on Armenian archaeological sites: fission-track dating of obsidians. Radiation Measurements 34, 373–378.
Badalyan, R., Chataigner, C., Kohl, P., 2004. Trans-caucasian obsidian: the exploitation of the sources and their distribution. In: Sagona, A. (Ed.), A View from the Highlands: Archaeological Studies in Honour of Charles Burney. Ancient Near Eastern Studies, pp. 437–465.
Blackman, M.J., Badalian, R., Kikodze, Z., Kohl, P., 1998. Chemical characterization of Caucasian obsidian geological sources. In: Cauvin, M.-C., Gourgaud, A., Gratuze, B., Arnaud, N., Poupeau, G., Poidevin, J.L., Chataigner, C. (Eds.), L'obsidienne au Proche et Moyen-Orient: Du Volcan à l'Outil, BAR International Series, pp. 205–231.
Brown, P.E., 1983. Tracing prehistoric sources of obsidian. In: Brown, P.E., Stone, C.L. (Eds.), Granite Reef: a Study in Desert Archaeology. Arizona State University, pp. 227–241.
Carter, T., Shackley, M., 2007. Sourcing obsidian from Neolithic çatalhöyük (Turkey) using energy dispersive X-ray fluorescence. Archaeometry 49, 437–454.
Cecil, L.G., Moriarty, M.D., Speakman, R.J., Glascock, M.D., 2007. Feasibility of field-portable XRF to identify obsidian sources in central Peten, Guatemala. In: Glascock, M.D., Speakman, R.J., Popelka-Filcoff, R.S. (Eds.), Archaeological Chemistry: Analytical Techniques and Archaeological Interpretation, ACS Symposium Series, vol. 968. American Chemical Society, Washington, DC, pp. 506–521.
Chataigner, C., Badalian, R., Bigazzi, G., Cauvin, M.-C., 2003. Provenance studies of obsidian artefacts from Armenian archaeological sites using the fission-track dating method. J. Non-Cryst. Solids 323, 172–179.
Chataigner, C., Barge, O., 2007. Quantitative approach to the diffusion of obsidian in the ancient northern near east. In: Conference on Computer Applications and Quantitative Methods in Archaeology (CAA), Berlin, Germany.
Chataigner, C., Gratuze, B., 2013a. New data on the exploitation of obsidian in the southern Caucasus (Armenia, Georgia) and Eastern Turkey, part 1: source characterization. Archaeometry. http://dx.doi.org/10.1111/arcm.12006.
Chataigner, C., Gratuze, B., 2013b. New data on the exploitation of obsidian in the southern Caucasus (Armenia, Georgia) and Eastern Turkey, part 2: obsidian procurement from the Upper Palaeolithic to the Late Bronze Age. Archaeometry. http://dx.doi.org/10.1111/arcm.12007.
Cherry, J.F., Faro, E.Z., Minc, L., 2010. Field survey and geochemical characterization of the southern Armenian obsidian sources. Journal of Field Archaeology 35 (2), 147–163.
Craig, N., Speakman, R.J., Popelka-Filcoff, R., Glascock, M.D., Robertson, J., Shackley, M.S., Aldenderfer, M., 2007. Comparison of XRF and PXRF for analysis of archaeological obsidian from southern Perú. J. Archaeol. Sci. 34, 2012–2024.

Craig, N., Speakman, R.J., Popelka-Filcoff, R., Aldenderfer, M., Blanco, L., Vega, M., Glascock, M.D., Stanish, C., 2010. Macusani obsidian from southern Peru: a characterization of its elemental composition with a demonstration of its ancient use. J. Archaeol. Sci. 37, 569–576.
De Francesco, A.M., Crisci, G.M., Bocci, M., 2008. Non-destructive analytic method using XRF for determination of provenance of archaeological obsidians from the Mediterranean Area: a comparison with traditional XRF methods. Archaeometry 50 (2), 337–350.
Dibble, H.L., Chase, P.G., McPherron, S.P., Tuffreau, A., 1997. Testing the reality of a "living floor" with archaeological data. Am. Antiq. 62 (4), 629–651.
Enloe, J.G., 2006. Geological processes and site structure: assessing integrity at a Late Paleolithic open-air site in northern France. Geoarchaeology 21, 523–540.
Ericson, J.E., Glascock, M.D., 2004. Subsource characterization: obsidian utilization of subsources of the Coso Volcanic Field, Coso Junction, California, USA. Geoarchaeology 19 (8), 779–805.
Feinman, G.M., Nicholas, L.M., Haines, H.R., 2007. Classic Period agricultural intensification and domestic life at El Palmillo, Valley of Oaxaca, Mexico. In: Thurston, T.L., Fisher, C.T. (Eds.), Seeking a Richer Harvest: the Archaeology of Subsistence Intensification, Innovation, and Change. Springer, pp. 23–62.
Forster, N., Grave, P., Vickery, N., Kealhofer, L., 2011. Non-destructive analysis using PXRF: methodology and application to archaeological ceramics. X-ray Spectrom. 40, 389–398.
Forster, N., Grave, P., 2012. Non-destructive PXRF analysis of museum-curated obsidian from the near east. J. Archaeol. Sci. 39, 728–736.
Frahm, E., 2012. Non-destructive sourcing of Bronze-Age near Eastern obsidian artefacts: redeveloping and reassessing electron microprobe analysis for obsidian sourcing. Archaeometry 54, 623–642.
Frahm, E., Doonan, R., Kilikoglou, V., 2013. Handheld portable X-ray fluorescence of Aegean obsidians. Archaeometry. http://dx.doi.org/10.1111/arcm.12012.
Freund, K.P., Tykot, R.H., 2011. Lithic technology and obsidian exchange networks in Bronze Age Nuragic Sardinia (Italy). Archaeol. Anthropol. Sci. 3 (2), 151–164.
Giauque, R.D., Asaro, F., Stross, F.H., Hester, T.R., 1993. High-precision non-destructive x-ray fluorescence method applicable to establishing the provenance of obsidian artifacts. X-ray Spectrom. 22, 44–53.
Glascock, M.D., 1992. Characterization of archaeological ceramics at MURR by neutron activation analysis and multivariate statistics. In: Neff, H. (Ed.), Chemical Characterization of Ceramic Pastes in Archaeology. Prehistory Press, Madison, pp. 11–26.
Glascock, M.D., Braswell, G., Cobean, R.H., 1998. A systematic approach to obsidian source characterization. In: Shackley, M.S. (Ed.), Archaeological Obsidian Studies: Method and Theory. Society for Archaeological Sciences, pp. 15–65.
Glascock, M.D., Speakman, R.J., Neff, H., 2007. Archaeometry at the University of Missouri Research Reactor and the provenance of obsidian artefacts in North America. Archaeometry 49, 343–357.
Godfrey-Smith, D.I., Haywood, N., 1984. Obsidian sources in Ontario Prehistory. Ont. Archaeol. 41, 29–35.
Golitko, M., Meierhoff, J., Terrell, J., 2010. Chemical characterization of sources of obsidian from the Sepik coast (PNG). Archaeol. Ocean. 45, 120–129.
Golitko, M., Schauer, M., Terrell, J.E., 2012. Identification of Fergusson Island obsidian on the Sepik coast of northern Papua New Guinea. Archaeol. Ocean. 47, 151–156.
Goodale, N., Bailey, D., Jones, G., Prescott, C., Scholz, E., Stagliano, N., Lewis, C., 2012. pXRF: a study of inter-instrument performance. J. Archaeol. Sci. 39, 875–883.
Harbottle, G., 1982. Chemical characterization in archaeology. In: Ericson, J., Earle, T.K. (Eds.), Contexts for Prehistoric Exchange. Academic Press, New York, pp. 13–51.
Hejzlar, Z., Pesce, J., 5–6 November 2009. Applications of portable X-ray fluorescence in problematic drywall investigations. In: Technical Symposium on Corrosive Imported Drywall. Florida Department of Health, Tampa, Florida.
Hughes, R.E., 1984. Obsidian studies in the Great Basin. In: Contributions of the University of California Archaeological Research Facility, vol. 45. University of California.
Hughes, R.E., 1998. On reliability, validity, and scale in obsidian sourcing research. In: Ramenofsky, A.F., Steffen, A. (Eds.), Unit Issues in Archaeology: Measuring Time, Space, and Material. University of Utah Press, Salt Lake City, Utah, pp. 103–114.
Jack, R.N., Carmichael, I.S.E., 1969. The Chemical "Fingerprinting" of Acid Volcanic Rocks. Short Contributions to California Geology: Special Report. California Division of Mines and Geology, pp. 17–32.
Jack, R.N., Heizer, R.F., 1968. "Finger-printing" of Some Mesoamerican Obsidian Artifacts. In: Contributions of the University of California Archaeological Research Facility, vol. 5, pp. 81–100.
Jia, P., Doelman, T., Chen, C., Zhao, H., Lin, S., Torrence, R., Glascock, M.D., 2010. Moving sources: a preliminary study of volcanic glass artifact distributions in northeast China using PXRF. J. Archaeol. Sci. 37, 1670–1677.
Karapetian, S.G., Bashian Jr., R., Mnatsakanian, A.Kh, 2001. Late collision rhyolitic volcanism in the north-eastern part of the Armenian Highland. J. Volcanol. Geotherm. Res. 112, 189–220.
Kasper, K., Pernicka, E., Kohl, P., 2004. Neutronenaktivierungsanalyse zur Herkunftsbestimmung Archäologischer Obsidianartefakte aus Aserbaidschan. In: Archäometrie und Denkmalpflege 2004, Jahrestagung in den Reiss-Engelhorn Museen Mannheim, 6–9 Oktober 2004.
Keller, J., Djerbashian, E., Pernicka, E., Karapetian, S., Nasedkin, V., 1996. Armenian and Caucasian obsidian occurrences as sources for the Neolithic Trade: volcanological setting and chemical characteristics. In: Archaeometry 94: the Proceedings of the 29th International Symposium on Archaeometry; Ankara, 9–14 May 1994, pp. 69–86.
Kelly, R.L., Thomas, D.H., 2012. Archaeology, sixth ed. Wadsworth, Cengage Learning.
Kuhn, S.L., 1995. Mousterian Lithic Technology. Princeton University Press.
Liritzis, I., 2008. Assessment of Aegean obsidian sources by a portable ED-XRF analyser: grouping, provenance and accuracy. In: Facorellis, Y., Zacharias, N., Polikreti, K., Vakoulis, T., Bassiakos, Y., Kiriatzi, V., Aloupi, E. (Eds.), Archaeometry Studies in the Aegean: Reviews and Recent Developments. Archaeopress, Oxford, pp. 399–406.
Liritzis, I., Zacharias, N., 2011. Portable XRF of archaeological artifacts: current research, potentials and limitations (Chapter 6). In: Shackley, M.S. (Ed.), X-ray Fluorescence Spectrometry (XRF) in Geoarchaeology. Springer, pp. 109–142.
Luedtke, B., 1992. An Archaeologist's Guide to Chert and Flint. In: Archaeological Research Tools, vol. 7. Institute of Archaeology, University of California-Los Angeles.
Lyman, R.L., 2009. Prehistory of the Oregon Coast: the Effects of Excavation Strategies and Assemblage Size on Archaeological Inquiry. Left Coast Press.
Machado, J., Hernández, C.M., Mallol, C., Galván, B., 2013. Lithic production, site formation and Middle Palaeolithic palimpsest analysis: in search of human occupation episodes at Abric del Pastor Stratigraphic Unit IV (Alicante, Spain). J. Archaeol. Sci. 40, 2254–2273.
Malinsky-Buller, A., Hovers, E., Marder, O., 2011. Making time: 'living floors', 'palimpsests' and site formation processes – a perspective from the open-air Lower Paleolithic site of Revadim Quarry, Israel. J. Anthropol. Archaeol. 30 (2), 89–101.
Mathieu, J.R., Scott, R.E. (Eds.), 2004. Exploring the Role of Analytical Scale in Archaeological Interpretation. BAR International Series, vol. 1261. Oxford.
McCoy, M., Mills, P., Lundblad, S., Rieth, T., Kahn, J., Gard, R., 2011. A cost surface model of volcanic glass quarrying and exchange in Hawai'i. J. Archaeol. Sci. 38, 2547–2560.
Meliksetian, Kh., Pernicka, E., Badalyan, R., Schifer, T., 2010. Geochemical characteristics of obsidian sources of the South Caucasus and provenance of Middle Palaeolithic to Early Iron Age obsidian artefacts. In: 38th International Symposium on Archaeometry, Tampa, Florida, United States, 10–14 May 2010.
Meliksetian, Kh, Pernicka, E., Schifer, T., Badalyan, R., Keller, J., Gasparyan, B., Karapetyan, S., Kunze, R., 2013. Trace Element Geochemistry of Armenian Obsidian Sources and Provenance of Archaeological Obsidian Artefacts. Veröff. Landesamtes Denkmalpflege u. Arch. Sachsen-Anhalt – Landesmus. Vorgesch (in press).
Merrick, H., Brown, F., 1984. Rapid chemical characterization of obsidian artifacts by electron microprobe analysis. Archaeometry 26 (2), 230–236.
Millhauser, J., Rodríguez-Alegría, E., Glascock, M.D., 2011. Testing the accuracy of portable X-ray fluorescence to study Aztec and colonial obsidian supply at Xaltocan, Mexico. J. Archaeol. Sci. 38, 3141–3152.
Nazaroff, A., Prufer, K., Drake, B., 2010. Assessing the applicability of portable X-ray fluorescence spectrometry for obsidian provenance research in the Maya lowlands. J. Archaeol. Sci. 37, 885–895.
Negash, A., Shackley, M.S., 2006. Geochemical provenance of obsidian artefacts from the MSA Site of Porc Epic, Ethiopia. Archaeometry 48 (1), 1–12.
Oddone, M., Bigazzi, G., Keheyan, Y., Meloni, S., 2000. Characterisation of Armenian obsidians: implications for raw material supply for prehistoric artifacts. J. Radioanal. Nucl. Chem. 243 (3), 673–682.
Phillips, S., Speakman, R.J., 2009. Initial source evaluation of archaeological obsidian from the Kuril Islands of the Russian Far East using portable XRF. J. Archaeol. Sci. 36, 1256–1263.
Rapp, G.R., Hill, C.L., 2006. Geoarchaeology: the Earth-science Approach to Archaeological Interpretation, second ed. Yale University Press, New Haven.
Seelenfreund, A., Miranda, J., Dinator, M., Morales, J., 2002. The provenance of archaeological obsidian artifacts from northern Chile determined by source-induced X-ray fluorescence. J. Radioanal. Nucl. Chem. 251 (1), 15–19.
Shackley, M.S., 1988. Sources of archaeological obsidian in the southwest: an archaeological, petrological, and geochemical study. Am. Antiq. 53 (4), 752–772.
Shackley, M.S., 1995. Sources of archaeological obsidian in the greater American southwest: an update and quantitative analysis. Am. Antiq. 60 (3), 531–551.
Shackley, M.S., 2005. Obsidian: Geology and Archaeology in the North American Southwest. University of Arizona.
Shackley, M.S., 2008. Archaeological petrology and the archaeometry of lithic materials. Archaeometry 50 (2), 194–215.
Shackley, M.S., 2009. Intersource and intrasource geochemical variability in two newly discovered archaeological obsidian sources in the southern Great Basin. J. Calif. Great Basin Anthropol. 16 (1), 118–129.
Shackley, M.S., 2011. An introduction to X-ray fluorescence (XRF) analysis in archaeology (Chapter 2). In: Shackley, M.S. (Ed.), X-ray Fluorescence Spectrometry (XRF) in Geoarchaeology. Springer, pp. 7–44.
Sheppard, P., Irwin, G., Lin, S., McCaffrey, C., 2011. Characterization of New Zealand obsidian using PXRF. J. Archaeol. Sci. 38, 45–56.
Silliman, S., 2005. Obsidian studies and the archaeology of 19th-century California. J. Field Archaeol. 30 (1), 75–94.
Sneath, P.H.A., Sokal, R.R., 1973. Numerical Taxonomy: the Principles and Practice of Numerical Classification. W. H. Freeman & Company.
Speakman, R.J., Shackley, M.S., 2013. Commentary: silo science and portable XRF in Archaeology: a response to Frahm. J. Archaeol. Sci. 40, 1435–1443.

Speakman, R.J., Holmes, C.E., Glascock, M.D., 2007. Source determination of obsidian artifacts from swan point (XBD- 156), Alaska. Curr. Res. Pleistocene 24, 143–145.

Tykot, R.H., 1995. Prehistoric Trade in the Western Mediterranean: the Sources and Distribution of Sardinian Obsidian (PhD dissertation). Harvard University.

Tykot, R.H., Lai, L., Tozzi, C., 2011. Intra-site obsidian subsource patterns at Contraguda, Sardinia (Italy). In: Turbanti-Memmi, I. (Ed.), Proceedings of the 37th International Symposium on Archaeometry. Springer, pp. 321–328.

Vázquez, C., Palacios, O., Lué-Mer, M., Custo, G., Ortiz, M., Murillo, M., 2011. Provenance study of obsidian samples by using portable and conventional X ray fluorescence spectrometers: performance comparison of both instrumentations. J. Radioanal. Nucl. Chem. 292 (1), 367–373.

Weisler, M.I., Clague, D.A., 1998. Characterisation of archaeological volcanic glass from oceania: the utility of three techniques. In: Shackley, M.S. (Ed.), Archaeological Obsidian Studies: Method and Theory. Society for Archaeological Sciences, pp. 103–128.